Research Article | Vol. 27, No. 8 | 15 Apr 2019 | OPTICS EXPRESS A364
Optics EXPRESS

Gallium Phosphide photoanode coated with TiO_2 and CoO_x for stable photoelectrochemical water oxidation

M. ALQAHTANI,[1,2,*] S. BEN-JABAR,[3,4] M. EBAID,[5] S. SATHASIVAM,[3] P. JURCZAK,[1] X. XIA,[3] A. ALROMAEH,[2] C. BLACKMAN,[3] Y. QIN,[6] B. ZHANG,[6] B. S. OOI,[5] H. LIU,[1] I. P. PARKIN,[3] AND J. WU[1,7,8]

[1]*Department of Electronic and Electrical Engineering, University College London, London WC1E 7JE, United Kingdom*
[2]*King Abdulaziz City for Science and Technology (KACST), Riyadh 12371, Saudi Arabia*
[3]*Department of Chemistry, University College London, London WC1H 0AJ, United Kingdom*
[4]*Department of Forensic Science, King Fahad Security College (KFSC), Riyadh 13232, Saudi Arabia*
[5]*King Abdullah University of Science and Technology (KAUST), Thuwal 23955- 6900, Saudi Arabia*
[6]*Institute of Coal Chemistry, Chinese Academy of Sciences, Taiyuan 030001, China*
[7]*Institute of Fundamental and Frontier Sciences, University of Electronic Science and Technology of China, Chengdu 610054, China*
[8]*jiangwu@uestc.edu.cn*
[*]*mahdi.alqahtani.16@ucl.ac.uk*

Abstract: Gallium Phosphide (GaP) has a band gap of 2.26 eV and a valance band edge that is more negative than the water oxidation level. Hence, it may be a promising material for photoelectrochemical water splitting. However, one thing GaP has in common with other III-V semiconductors is that it corrodes in photoelectrochemical reactions. Cobalt oxide (CoO_x) is a chemically stable and highly active oxygen evolution reaction co-catalyst. In this study, we protected a GaP photoanode by using a 20 nm TiO_2 as a protection layer and a 2 nm cobalt oxide co-catalyst layer, which were both deposited *via* atomic layer deposition (ALD). A GaP photoanode that was modified by CoO_x exhibited much higher photocurrent, potential, and photon-to-current efficiency than a bare GaP photoanode under AM1.5G illumination. A photoanode that was coated with both TiO_2 and CoO_x layers was stable for over 24 h during constant reaction in 1 M NaOH (pH 13.7) solution under one sun illumination.

1. Introduction

The use of photoelectrochemcial (PEC) water splitting to harvest intermittent solar sources in the form of hydrogen is an attractive potential method to address the energy and environmental issues. Since Honda and Fujishima in 1972 demonstrated titanium dioxide (TiO_2) for PEC water splitting [1], extensive efforts have been devoted to the development of photoelectrodes with good stability and high solar-to-hydrogen efficiency. Metal oxides (e.g., TiO_2, Fe_2O_3, $BiVO_4$, and $SrTiO_2$) have been extensively studied but their wide band gap and sluggish charge transfer kineties typically limited their solar-to-hydrogen conversion efficiency [1–4]. III-V semiconductor materials have attracted for PEC water splitting due to their high-efficiency, optimal band gap, and excellent optical properties but are readily susceptible to corrosion in strongly acidic or basic aqueous solutions during PEC process [5–11]. Of III-V semiconductor materials, gallium phosphide (GaP) has an appropriate band gap of 2.26 eV for harvesting a large portion of solar energy and has a valence-band edge more negative than the water oxidation potential [5,12]. Although GaP-based photocathodes has been extensively studied [9,10,13,14], only relatively few studies demonstrated water

#352344 https://doi.org/10.1364/OE.27.00A364
Journal © 2019 Received 21 Nov 2018; revised 21 Jan 2019; accepted 23 Jan 2019; published 18 Mar 2019

oxidation using GaP photoanodes due to the challenges presented, which also include a requirement for high overpotential due to slow hole-transfer kinetics [5]. Recently, amorphous TiO_2 has been widely used to protect III-V photoelectrodes in combination with OER catalysts during water oxidation. For example, a leaky TiO_2 (~143 nm) coupled with Ni catalyst to stabilize the GaP photoanode and was achieved up to 6 h stability in 1M KOH [5]. In contrast, the earth-abundant CoO_x is effective for both functions, enhancing the oxygen evolution and stabilizing photoanodes, because it possesses efficient hole-conductivity and high resistance to photocorrosion under highly alkaline media [15]. Many studies have demonstrated highly active CoO_x as a co-catalyst for photoanodes. For instance, a silicon photoanode coated with ultra-thin CoO_x via atomic layer deposition (ALD) exhibited high stability for 24 h in 1 M NaOH [16], and a $BiVO_4$ photoanode coated with 2 nm CoO_x has shown stable photocurrent density in KOH solution [17]. By using amorphous TiO_2 as a protection layer and a layer made of highly active oxygen evolution reaction (OER) catalysts could further improve the stability of photoelectrodes under extreme pH conditions. Photocarriers is transferred to the solution via mid-gap states of a leaky amorphous TiO_2 layer and facilitated by the Cobalt Oxide (CoO_x) co-catalyst for water oxidation [18]. In this work, a 20 nm amorphous TiO_2 thin film was deposited as protection layer followed by ~2 nm cobalt oxide (CoO_x) as a co-catalyst both deposited *via* ALD on GaP surface. The GaP/TiO_2/CoO_x photoanode exhibited good stability for 24 hours in 1 M NaOH (pH 13.7) electrolyte under simulated one sun illumination. The GaP/TiO_2/CoO_x photoanode provides increased photocurrent density and improved onset potential compared to the reference GaP photoanode, ascribed to the high catalytic activity of cobalt oxide which is in agreement with previous reports [16,17,19].

2. Experiments

A GaP photoanode modified CoO_x was fabricated as follows: firstly, a single-crystalline n-GaP substrate was immersed in HCl solution (50% v/v) for 45 s, and then washed with deionized water followed by drying with N_2 gas. The dried sample was then transferred to an ALD chamber. An amorphous layer of TiO_2 with ~20 nm thickness was deposited directly onto the GaP electrode at 150 °C using a home-built ALD reactor by using titanium isopropoxide (TTIP) and water as metal and oxygen precursors respectively [20]. TTIP was kept at room temperature (25 °C) while water was kept at 5 °C. The deposition temperature was maintained at 150 °C. The growth rate of ALD process was approximately 0.4 Å/cycle. Following this, ALD of CoO_x layer (~2 nm) was deposited onto the TiO_2 layer at 250 °C [21,22]. X-ray Photoelectron Spectroscopy (XPS) was performed on a Thermo monochromated aluminium K-alfa photoelectron spectrometer, using monochromic Al-Kα radiation (1486.7 eV). Low resolution survey scans were measured between 0 and 1300 eV and high-resolution scans were used to measure O 1s, Ti 2p and Co 2p spectra to determine oxidation and elemental concentration. All spectra were calibrated to adventitious carbon at 284.5 eV and data was analyzed using CasaXPS software. To produce simulated sunlight, a 200W Xe arc lamp was used as a light source with AM 1.5 G filter. A calibrated silicon solar cell was used to calibrate the illumination intensity. The PEC performances were conducted in a three-electrode system using the photoanode as a working electrode, Ag/AgCl reference electrode and platinum coil as a counter electrode in 1 M NaOH solution (pH 13.7). The linear sweep voltammetry measurements were conducted by using a potentiostat (Ivium CompactStat). The incident-photon-to-current conversion efficiency (IPCE) and the applied bias photon-to-current efficiency (ABPE) was measured using a published procedure (19).

The AFM images were acquired with a Veeco Dimension V Scanning Probe Microscope with tapping mode at atmospheric pressure with a Si cantilever with 10 nm of radius. Gas evolution measurements were conducted in a leak-tight glass reactor with a quartz window, in a three-electrode PEC cell configuration where the GaP/TiO_2/CoO_x electrode acted as the photoanode with a Pt coil counter electrode and a Ag / AgCl reference electrode in 1 M

Optics EXPRESS

NaOH (pH 13.7) electrolyte. The reactor was connected to a high purity nitrogen gas circulation system to purge the reactor before illumination. The oxygen gas produced during the water splitting experiment was collected and quantified using SRI 310c gas chromatograph (GC) with a molecular sieve (5A) column and helium as the carrier gas.

3. Results and discussion

A schematic illustration of the GaP electrode modified by amorphous TiO_2 and cobalt oxide CoO_x are shown in Fig. 1(a). XPS measurements on the GaP photoanode was used to confirm the deposition of TiO_2 and CoO_x films, as shown in Figs. 1(b)-1(c). Figure 1(b) shows the Ti 2p ionisation with the Ti $2p_{3/2}$ peak centered at 458.1 eV, corresponding to TiO_2 [23]. The Co $2p_{3/2}$ spectrum was deconvoluted to five fitting peaks using the parameters given by Biesinger et al [24]. The principle peak at 780.0 eV matches well with that expected for a Co_3O_4/CoO layer [24]. It should also be noted that no Ga and no P were observable, suggesting the material is pinhole free.

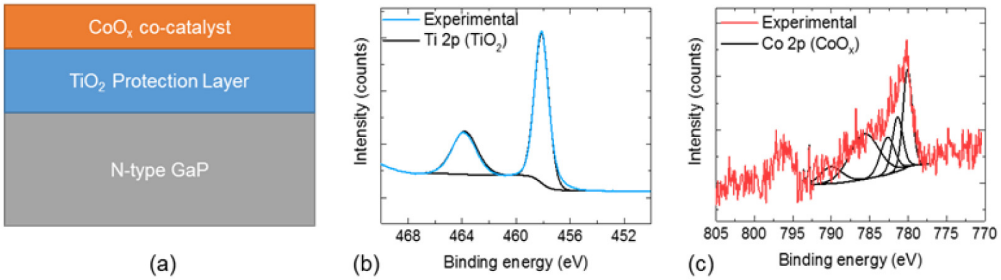

Fig. 1. (a) Schematic illustration of the GaP photoanode modified by amorphous TiO_2 and cobalt oxide CoO_x. 1(b) XPS spectra showing the Ti 2p and Co 2p spectra measured on the surface of the GaP/TiO_2/CoO_x photoanode pre-PEC analysis.

Atomic Force Microscopy (AFM) has been used to assess the surface morphology for the GaP/TiO_2/CoO_x photoanode. Figures 2(a)-2(c) shows AFM images of a planar view of the GaP/TiO_2/CoO_x photoanode surface and a 3D representation of the surface morphology. This measurement shows that the top CoO_x layer is a smooth thin film. The root-mean-square (rms) surface roughness of the GaP/TiO_2/CoO_x photoanode has been measured at 0.2 nm confirming high quality of the top layer.

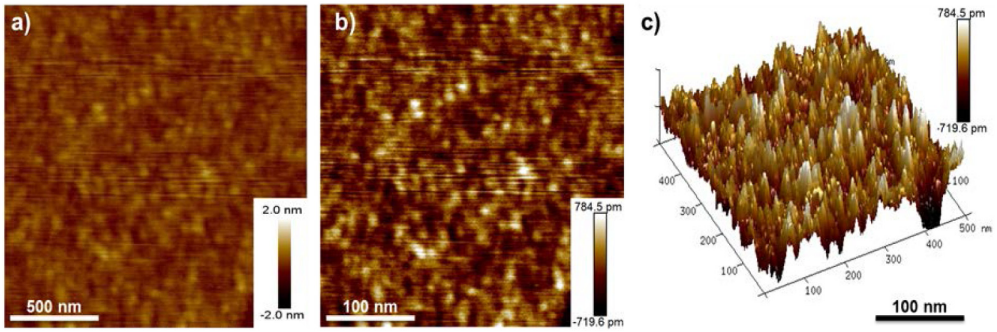

Fig. 2. Atomic force microscopy images morphology for the photoanode surface. Figures 2(a) and 2(b) Surface morphology of GaP-TiO_2/CoO_x photoanode. 2(c) 3D surface morphology of GaP-TiO_2/CoO_x. The z-scale is 2 nm and 784.5 pm for the AFM images in 2(a) and 2(b) respectively.

The current–voltage ($J-V$) characteristics for both GaP/TiO_2/CoO_x and bare GaP photoanodes are shown in Fig. 3(a). The bare GaP photoanode here was used a reference and exhibited an onset potential of −1 V and a photocurrent density of 0.19 mA/cm^2 at 0.5 V

Optics EXPRESS

versus reference electrode (Ag / AgCl). By comparison, GaP/TiO_2/CoO_x photoelectrode shows a great improvement in onset potential and photocurrent density, with the photocurrent was increased to around 0.788 mA/cm^2 at 0.5 V versus reference electrode Ag / AgCl in 1 M NaOH solution (pH 13.7) and the onset potential observed to be approximately −1.12 V. The improvement in photocurrent and onset potential could be attributed to enhance the charge transfer to semiconductor/electrolyte interface and the cobalt oxide activities. The PEC performance of the GaP photoanodes with respect to the applied potential was examined; the applied bias photon-to-current efficiency (ABPE) are shown in Fig. 3(b), with the peak ABPE values, measured at 0.5 V, for bare GaP and GaP/TiO_2/CoO_x photoanodes being 0.14% and 0.57% versus reference electrode (Ag / AgCl), respectively. The higher ABPE value for the GaP/TiO_2/CoO_x photoanode indicates the enhancement of hole collection and water oxidation likely due to the CoO_x-based catalysts. Similar to NiO_x, CoO_x is a highly active OER catalyst in a strong alkaline solution due to its relatively high CB edge and hence excellent hole-transfer property [15]. Moreover, the Ni and Co OER catalysts can result in oxyhydroxides on their surface, e.g. NiOOH and CoOOH, which can reduce the overpotential for OER activity [25,26].

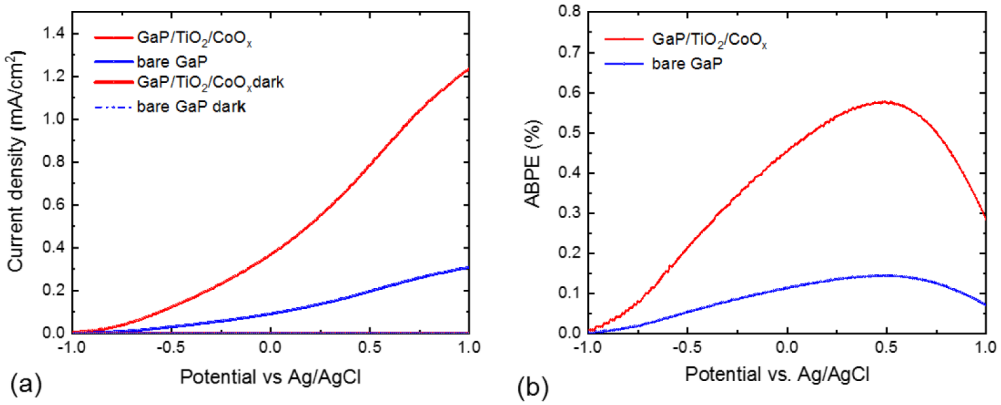

Fig. 3. Photoelectrochemical properties of GaP photoanodes. 3(a) The current-potential curves under AM 1.5G-simulated sunlight using three-electrode configuration in 1 M NaOH electrolyte (pH 13.7). 3(b) Applied bias photon-to-current efficiency (ABPE) for GaP photoanodes.

To further investigate the wavelength-dependent photoelectrochemical contribution of GaP photoanode to the photocurrent, the incident-photon-to-current conversion efficiency (IPCE) was measured. As shown in Fig. 4(a), the maximum IPCE achieved at wavelength 400 nm for the GaP/TiO_2/CoO_x photoanode was 44.6%, which is higher than the value of the bare GaP photoanode 34.2%. Moreover, the IPCE up to 36% between (350-450 nm) for the GaP/TiO_2/CoO_x photoanode whereas the IPCE value of the bare GaP photoanode was 28.3% which indicates the improved efficiencies of carrier separation and collection while using TiO_2 protection layer and CoO_x as a co-catalyst. The IPCE value decreases below 26.7% for GaP/TiO_2/CoO_x and 19.8% for bare GaP at the wavelength of 450 nm and further decreases towards longer wavelengths (> 500 nm). Marginal photoresponse was measured for the wavelength range from 500 to 550 nm while the absorption spectrum of the GaP/TiO_2/CoO_x extended to 550 nm. This is attributed to the indirect nature of GaP bandgap [9,13,27].

Oxygen production was evaluated for the GaP/TiO_2/CoO_x photoanode at zero V vs a reference electrode (Ag / AgCl) under AM 1.5G-simulated sunlight as shown in Fig. 4(b). The amount of gas produced during approximately 2 hours was collected and analysed using a gas chromatography system. The GaP/TiO_2/CoO_x photoanode showed increased oxygen evolution with time. An amount of approximately 0.15 mmol/cm^2 of oxygen was produced

Optics EXPRESS

after 2 hours of continuous irradiation, indicating an efficient water oxidation process. The advantage of the CoO_x-based catalyst can be clearly seen from the improved PEC water splitting stability and the improved $J-V$ curve of the the $GaP/TiO_2/CoO_x$ photoanode.

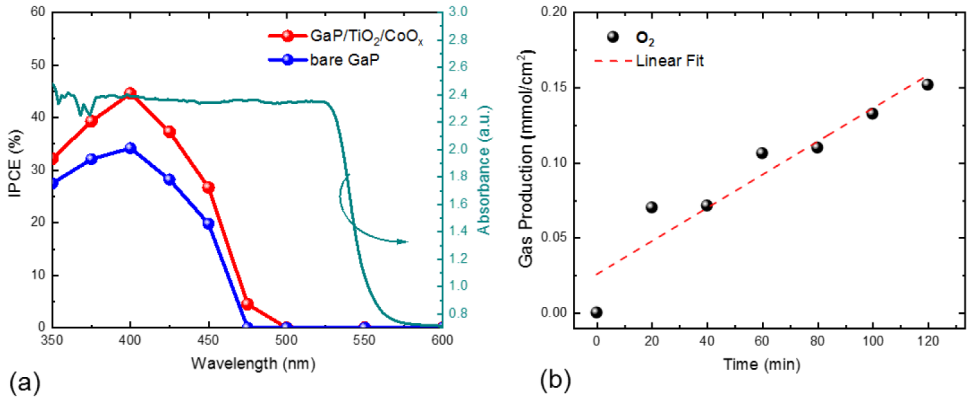

Fig. 4. (a) Incident photon-to-current conversion efficiency (IPCE) of $GaP/TiO_2/CoO_x$ photoanode in 1M NaOH electrolyte at 1 V versus Ag/AgCI. 4(b) Gas chromatography of the oxygen evolved from $GaP/TiO_2/CoO_x$ photoanode. The photoanode was biased at zero V versus reference electrode Ag/AgCl under AM 1.5G-simulated sunlight in 1 M NaOH solution.

The stability of the photoanode was studied by performing current density versus time ($J-t$) measurements. The photocurrent density of the $GaP/TiO_2/CoO_x$ photoanode was evaluated for 24 h using chronoamperometry at a fixed potential of zero bias V vs ($Ag/AgCl$) in 1 M NaOH solution. As shown in Fig. 5, the photocurrent is stable for 24 hours under continuous illumination for $GaP/TiO_2/CoO_x$ photoanode with marginal degradation. Clearly, the cobalt oxide catalyst along with the TiO_2 layer shows good stability because the TiO_2 layer has excellent hole-conducting and is chemical resistant under strongly basic electrolyte while cobalt oxides effectively transfer holes for water oxidation [15,28].

XPS analysis of the $GaP/TiO_2/CoO_x$ photoanodes was used to probe the surface chemistry after the long stability test as shown in Figs. 5(b)-5(c). Before PEC analysis, only peaks for Co, and Ti were observed on the surface as shown in Figs. 1(b)-1(c). After PEC, the intensity of the Co 2p peaks are reduced (as evidenced by the low signal to noise ratio) but still visible therefore indicating the presence of the CoO_x layer even after exposure to the harsh electrolyte. Again, similar to CoO_x, the TiO_2 layer was still intact after 24 hours of exposure to the strongly basic solution as a Ti 2p signal was still seen with the $Ti2p_{3/2}$ peak at 457.9 eV, matching Ti in the 4 + oxidation state. Despite the CoO_x and TiO_2 layers being present, a spectrum for P 2p was measured, this was most likely due to possible diffusion of P through the TiO_2 and CoO_x layers or formation of pinholes after PEC experiment.

Optics EXPRESS

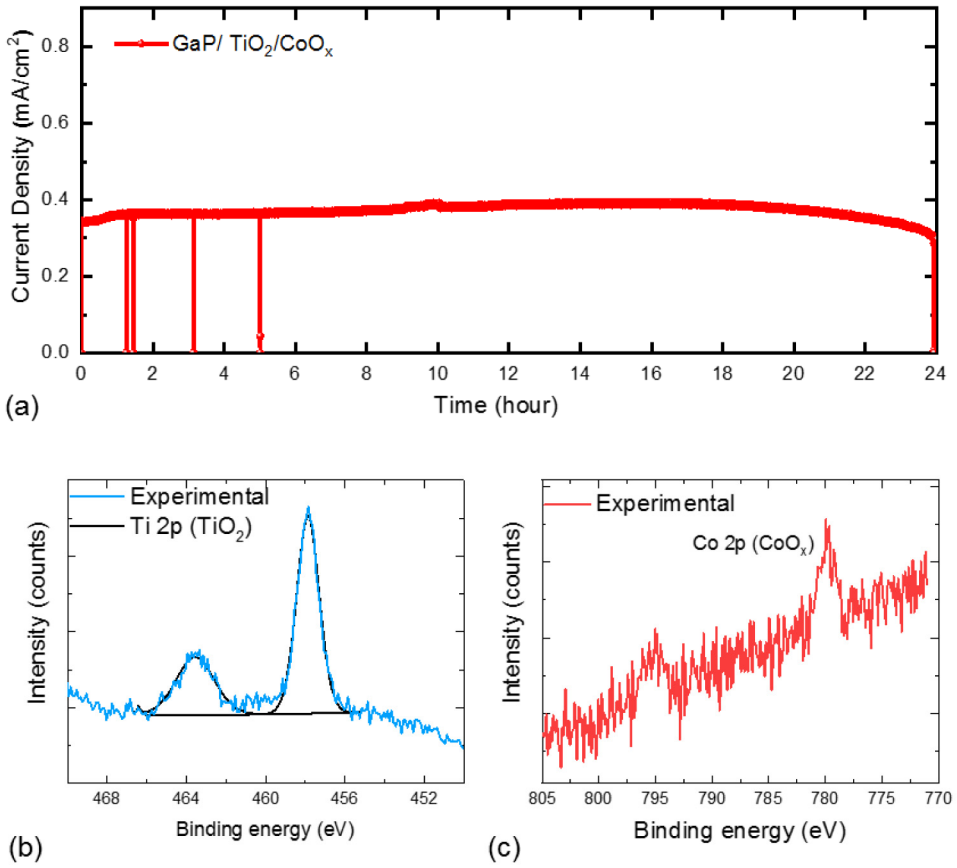

Fig. 5. Stability and Chemical properties of GaP/TiO_2/CoO_x photoanodes. 5(a) Steady-state photocurrent of the GaP photoanode held at zero V versus reference electrode (Ag/AgCl) under simulated one sunlight. 5(b) XPS spectra showing the Ti 2p (b) and Co 2p. 5(c) transitions from the surface of the photoanode after the reliability test for 24 hours.

4. Conclusion

In conclusion, we have deposited a TiO_2-protection layer along with an ultra-thin layer of cobalt oxides as an OER catalyst on a GaP photoanode by ALD. The TiO_2/CoO_x improved the activity and increased the stability of the GaP photoanode for 24 h in 1 M NaOH (pH 13.7) solution under the AM 1.5G simulated solar light irradiation. Moreover, the GaP/TiO_2/CoO_x photoanode provides increased photocurrent density, improved onset potential, and incident-photon-to-current conversion efficiency (IPCE) compared to a bare GaP photoanode due to the high catalytic activity and corrosion resistant of cobalt oxide.

Funding

This work is supported by King Abdulaziz City for Science and Technology (KACST), Riyadh, Saudi Arabia. The Future Compound Semiconductor Manufacturing Hub (CS Hub) funded by EPSRC grant EP/P006973/1.

Acknowledgements

M.A. and J.W. conceived the idea and wrote the manuscript. M.A. performed the PEC experiments and analysed the data. S.S. performed XPS and related analysis. S. B. conducted Ultraviolet–visible spectroscopy (UV–Vis) and related analysis. P.J. performed AFM and related analysis. ALD CoO_x was grown by B.Z. and Y.Q. X. X. and C. B. performed ALD

Optics EXPRESS

TiO_2. M. E. and B. O. measured the gas evolution. All authors reviewed and commented on the manuscript.

References

1. A. Fujishima and K. Honda, "Electrochemical photolysis of water at a semiconductor electrode," Nature **238**(5358), 37–38 (1972).
2. D. K. Lee and K.-S. Choi, "Enhancing long-term photostability of BiVO4 photoanodes for solar water splitting by tuning electrolyte composition," Nat. Energy **3**(1), 53–60 (2018).
3. K. Iwashina and A. Kudo, "Rh-doped SrTiO3 photocatalyst electrode showing cathodic photocurrent for water splitting under visible-light irradiation," J. Am. Chem. Soc. **133**(34), 13272–13275 (2011).
4. D. K. Zhong, J. Sun, H. Inumaru, and D. R. Gamelin, "Solar water oxidation by composite catalyst/alpha-Fe(2)O(3) photoanodes," J. Am. Chem. Soc. **131**(17), 6086–6087 (2009).
5. S. Hu, M. R. Shaner, J. A. Beardslee, M. Lichterman, B. S. Brunschwig, and N. S. Lewis, "Amorphous TiO(2) coatings stabilize Si, GaAs, and GaP photoanodes for efficient water oxidation," Science **344**(6187), 1005–1009 (2014).
6. J. Wu, Y. Li, J. Kubota, K. Domen, M. Aagesen, T. Ward, A. Sanchez, R. Beanland, Y. Zhang, M. Tang, S. Hatch, A. Seeds, and H. Liu, "Wafer-scale fabrication of self-catalyzed 1.7 eV GaAsP core-shell nanowire photocathode on silicon substrates," Nano Lett. **14**(4), 2013–2018 (2014).
7. J. L. Young, K. X. Steirer, M. J. Dzara, J. A. Turner, and T. G. Deutsch, "Remarkable stability of unmodified GaAs photocathodes during hydrogen evolution in acidic electrolyte," J. Mater. Chem. A Mater. Energy Sustain. **4**(8), 2831–2836 (2016).
8. F. Yang, A. C. Nielander, R. L. Grimm, and N. S. Lewis, "Photoelectrochemical Behavior of n-Type GaAs(100) Electrodes Coated by a Single Layer of Graphene," J. Phys. Chem. C **120**(13), 6989–6995 (2016).
9. M. Malizia, B. Seger, I. Chorkendorff, and P. C. K. Vesborg, "Formation of a p–n heterojunction on GaP photocathodes for H2production providing an open-circuit voltage of 710 mV," J. Mater. Chem. A Mater. Energy Sustain. **2**(19), 6847–6853 (2014).
10. A. Standing, S. Assali, L. Gao, M. A. Verheijen, D. van Dam, Y. Cui, P. H. Notten, J. E. Haverkort, and E. P. Bakkers, "Efficient water reduction with gallium phosphide nanowires," Nat. Commun. **6**(1), 7824 (2015).
11. J. Gu, J. A. Aguiar, S. Ferrere, K. X. Steirer, Y. Yan, C. Xiao, J. L. Young, M. Al-Jassim, N. R. Neale, and J. A. Turner, "A graded catalytic–protective layer for an efficient and stable water-splitting photocathode," Nat. Energy **2**(2), 16192 (2017).
12. M. G. Walter, E. L. Warren, J. R. McKone, S. W. Boettcher, Q. Mi, E. A. Santori, and N. S. Lewis, "Solar water splitting cells," Chem. Rev. **110**(11), 6446–6473 (2010).
13. S. Lee, A. R. Bielinski, E. Fahrenkrug, N. P. Dasgupta, and S. Maldonado, "Macroporous p-GaP photocathodes prepared by anodic etching and atomic layer deposition doping," ACS Appl. Mater. Interfaces **8**(25), 16178–16185 (2016).
14. C. Liu, J. Sun, J. Tang, and P. Yang, "Zn-doped p-type gallium phosphide nanowire photocathodes from a surfactant-free solution synthesis," Nano Lett. **12**(10), 5407–5411 (2012).
15. D. Bae, B. Seger, P. C. Vesborg, O. Hansen, and I. Chorkendorff, "Strategies for stable water splitting via protected photoelectrodes," Chem. Soc. Rev. **46**(7), 1933–1954 (2017).
16. J. Yang, K. Walczak, E. Anzenberg, F. M. Toma, G. Yuan, J. Beeman, A. Schwartzberg, Y. Lin, M. Hettick, A. Javey, J. W. Ager, J. Yano, H. Frei, and I. D. Sharp, "Efficient and sustained photoelectrochemical water oxidation by cobalt oxide/silicon photoanodes with nanotextured interfaces," J. Am. Chem. Soc. **136**(17), 6191–6194 (2014).
17. M. F. Lichterman, M. R. Shaner, S. G. Handler, B. S. Brunschwig, H. B. Gray, N. S. Lewis, and J. M. Spurgeon, "Enhanced stability and activity for water oxidation in alkaline media with bismuth vanadate photoelectrodes modified with a cobalt oxide catalytic layer produced by atomic layer deposition," J. Phys. Chem. Lett. **4**(23), 4188–4191 (2013).
18. Y. W. Chen, J. D. Prange, S. Dühnen, Y. Park, M. Gunji, C. E. Chidsey, and P. C. McIntyre, "Atomic layer-deposited tunnel oxide stabilizes silicon photoanodes for water oxidation," Nat. Mater. **10**(7), 539–544 (2011).
19. M. Alqahtani, S. Sathasivam, A. Alhassan, F. Cui, S. BenJaber, C. Blackman, B. Zhang, Y. Qin, I. P. Parkin, S. Nakamura, H. Liu, and J. Wu, "InGaN/GaN multiple quantum well photoanode modified with cobalt oxide for water oxidation," ACS Applied Energy Materials **1**(11), 6417–6424 (2018).
20. R. L. Wilson, C. E. Simion, C. S. Blackman, C. J. Carmalt, A. Stanoiu, F. Di Maggio, and J. A. Covington, "The effect of film thickness on the gas sensing properties of ultra-thin TiO(2) films deposited by atomic layer deposition," Sensors (Basel) **18**(3), 735 (2018).
21. J. Zhang, Z. Yu, Z. Gao, H. Ge, S. Zhao, C. Chen, S. Chen, X. Tong, M. Wang, Z. Zheng, and Y. Qin, "Porous TiO_2 nanotubes with spatially separated platinum and CoO_x cocatalysts produced by atomic layer deposition for photocatalytic hydrogen production," Angew. Chem. Int. Ed. Engl. **56**(3), 816–820 (2017).
22. Y. Q. Li, S. C. Zhao, Q. M. Hu, Z. Gao, Y. Q. Liu, J. K. Zhang, and Y. Qin, "Highly efficient CoOx/SBA-15 catalysts prepared by atomic layer deposition for the epoxidation reaction of styrene," Catal. Sci. Technol. **7**(10), 2032–2038 (2017).

Optics EXPRESS

23. M. C. Biesinger, L. W. M. Lau, A. R. Gerson, and R. S. C. Smart, "Resolving surface chemical states in XPS analysis of first row transition metals, oxides and hydroxides: Sc, Ti, V, Cu and Zn," Appl. Surf. Sci. **257**(3), 887–898 (2010).
24. M. C. Biesinger, B. P. Payne, A. P. Grosvenor, L. W. M. Lau, A. R. Gerson, and R. S. Smart, "Resolving surface chemical states in XPS analysis of first row transition metals, oxides and hydroxides: Cr, Mn, Fe, Co and Ni," Appl. Surf. Sci. **257**(7), 2717–2730 (2011).
25. L. Trotochaud, S. L. Young, J. K. Ranney, and S. W. Boettcher, "Nickel-iron oxyhydroxide oxygen-evolution electrocatalysts: the role of intentional and incidental iron incorporation," J. Am. Chem. Soc. **136**(18), 6744–6753 (2014).
26. M. S. Burke, M. G. Kast, L. Trotochaud, A. M. Smith, and S. W. Boettcher, "Cobalt-iron (oxy)hydroxide oxygen evolution electrocatalysts: the role of structure and composition on activity, stability, and mechanism," J. Am. Chem. Soc. **137**(10), 3638–3648 (2015).
27. D. Khusnutdinova, A. M. Beiler, B. L. Wadsworth, S. I. Jacob, and G. F. Moore, "Metalloporphyrin-modified semiconductors for solar fuel production," Chem. Sci. (Camb.) **8**(1), 253–259 (2017).
28. E. Nurlaela, H. Wang, T. Shinagawa, S. Flanagan, S. Ould-Chikh, M. Qureshi, Z. Mics, P. Sautet, T. Le Bahers, E. Canovas, M. Bonn, and K. Takanabe, "Enhanced kinetics of hole transfer and electrocatalysis during photocatalytic oxygen evolution by cocatalyst tuning," ACS Catal. **6**(7), 4117–4126 (2016).